Organic & Biomolecular Chemistry

PAPER

View Article Online
View Journal | View Issue

Cite this: *Org. Biomol. Chem.*, 2014, **12**, 4691

B-DNA structure and stability: the role of hydrogen bonding, π–π stacking interactions, twist-angle, and solvation†

Jordi Poater,[a] Marcel Swart,[b,c] F. Matthias Bickelhaupt[a,d] and Célia Fonseca Guerra*[a]

Received 24th February 2014,
Accepted 20th May 2014

DOI: 10.1039/c4ob00427b

www.rsc.org/obc

We have computationally investigated the structure and stability of B-DNA. To this end, we have analyzed the bonding in a series of 47 stacks consisting of two base pairs, in which the base pairs cover the full range of natural Watson–Crick pairs, mismatched pairs, and artificial DNA base pairs. Our analyses provide detailed insight into the role and relative importance of the various types of interactions, such as, hydrogen bonding, π–π stacking interactions, and solvation/desolvation. Furthermore, we have analyzed the functionality of the twist-angle on the stability of the structure. Interestingly, we can show that all stacked base pairs benefit from a stabilization by 6 to 12 kcal mol^{-1} if stacked base pairs are twisted from 0° to 36°, that is, if they are mutually rotated from a congruent superposition to the mutually twisted stacking configuration that occurs in B-DNA. This holds especially for stacked AT pairs but also for other stacked base pairs, including GC. The electronic mechanism behind this preference for a twisted arrangement depends on the base pairs involved. We also show that so-called "diagonal interactions" (or cross terms) in the stacked base pairs are crucial for understanding the stability of B-DNA, in particular, in GC-rich sequences.

Introduction

Stacking interactions play a central role in determining the structure and stability of DNA, as follows from various computational studies.[1,2] Recently, we revealed the importance of π–π stacking as well solvent effects for the immensely high fidelity with which DNA replication occurs.[2] This study consisted of the first high-level quantum chemical study on DNA replication covering not only the formation of DNA base pairs but also π–π stacking interactions in a model system consisting of four DNA bases. We showed that the intrinsic affinity of the template-primer complex to select the correct natural DNA base derives from the concerted action of hydrogen-bonding patterns, (de)solvation effects, twist angle and π–π stacking interactions.[2] It was shown how π–π stacking plays a less pronounced role for the selectivity, but it is important for the overall stability of the aggregate of incoming nucleotide and the template-primer complex.

In the present work, we wish to gain more insight in the stability of the structure of B-DNA with high-level quantum chemical computations. It is known that the stability of the double helical structure of B-DNA is supplied by the hydrogen bonds as proposed by Watson and Crick[3] and by the stacking interactions. However, the relative importance of both stabilizing interactions as well as how they interfere with each other is largely unknown. The hydrogen bonds in Watson–Crick base pairs and mismatches thereof were shown to posses both electrostatic and covalent (*i.e.*, orbital interaction) character with reinforcement by π polarization.[4] More recently,[5] a series of Watson–Crick base pairs and mismatched DNA base pairs were analyzed in order to obtain a better comprehension of the hydrogen-bonding mechanism under aqueous solvation (see Scheme 1). This work also considered tautomerization, which might occur in aqueous conditions.[6] The lactim forms of guanine (G*) or thymine (T*), as well as the imino forms of cytosine (C*) or adenine (A*) were paired with a complementary natural base.[7]

In addition, the pairs formed with an isostere of T, 2,4-difluorotoluene (F) were also taken into account. Kool *et al.*[8] demonstrated experimentally that F can be correctly incorporated into template-primer complexes, forming A–F pairs, in the presence of DNA polymerase. This finding was

[a]*Department of Theoretical Chemistry and Amsterdam Center for Multiscale Modeling, VU University Amsterdam, De Boelelaan 1083, NL-1081 HV Amsterdam, The Netherlands. E-mail: C. FonsecaGuerra@vu.nl*
[b]*Institut de Química Computacional i Catàlisi and Departament de Química, Universitat de Girona, 17071 Girona, Catalonia, Spain*
[c]*Institució Catalana de Recerca i Estudis Avançats (ICREA), Pg. Lluís Companys 23, 08010 Barcelona, Spain*
[d]*Institute of Molecules and Materials, Radboud University Nijmegen, Heyendaalseweg 135, 6525 AJ Nijmegen, The Netherlands*

†Electronic supplementary information (ESI) available: Stacking interaction energies and energy decomposition analyses of some stacked base pairs enclosed. See DOI: 10.1039/c4ob00427b

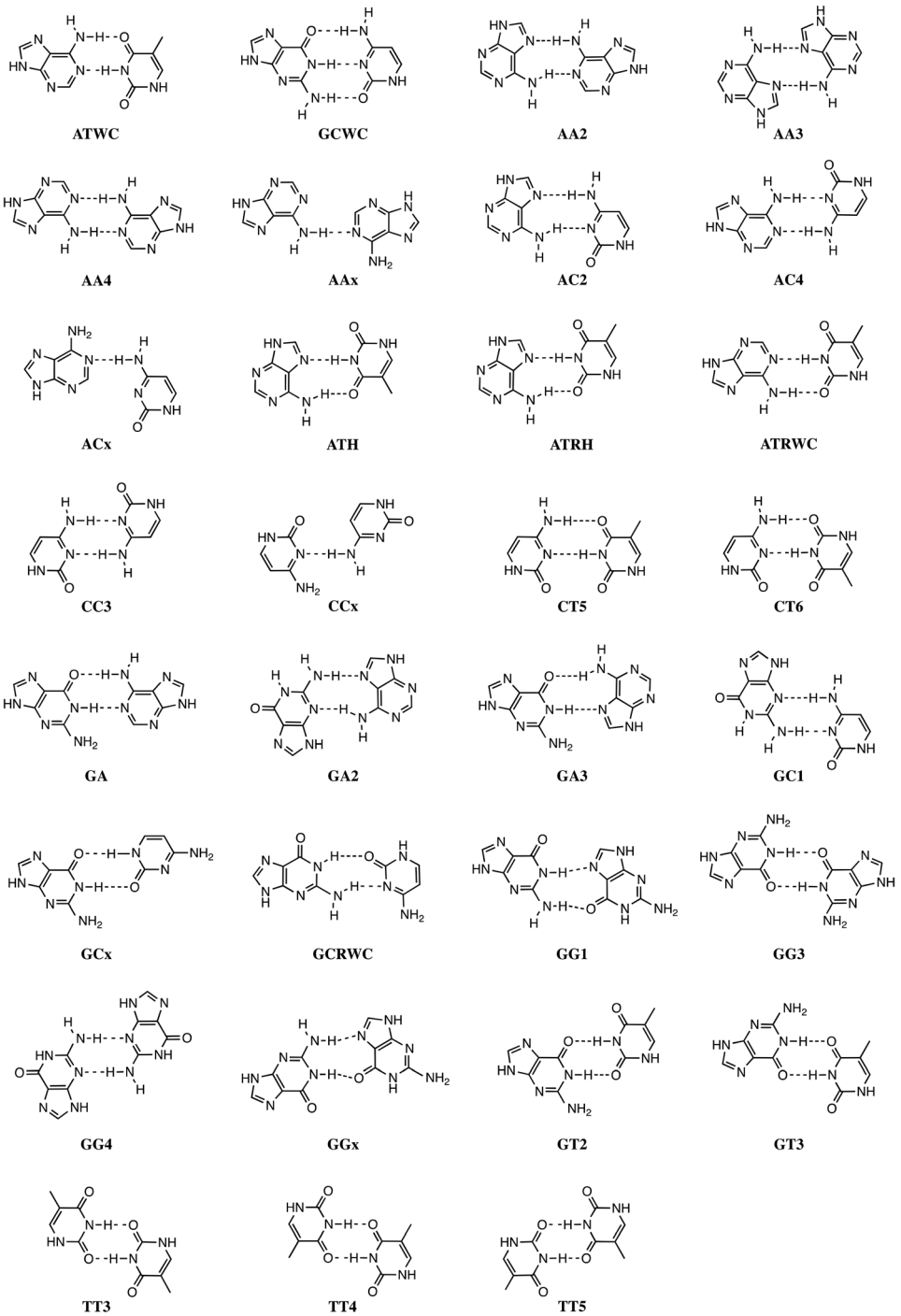

Scheme 1 Watson–Crick and mismatched base pairs.

explained computationally with the presence of the attractive donor–acceptor interactions in the weak hydrogen bonding.[9] The charge transfer interactions relieve the repulsive interaction when the A–F pair is confined to the spatial pocket of the polymerase. Finally, also the pairing of 5-chlorouracil paired with A was studied (see Scheme 2).[5] This mimic of uracil has recently been found[10] by Marlière *et al.* to correctly incorporate into an *Escherichia coli* strain with the posterior survival of the bacteria without the need of the initial T. From previous work, we know that in the condensed phase all hydrogen bonds of the base pairs become weaker and most of these bonds elongate. This can be explained by the stabilization of the lone pairs in the separate bases involved in hydrogen bonding.

Thus, herein, we want to incorporate the stacking interactions into our computational investigations and analyze

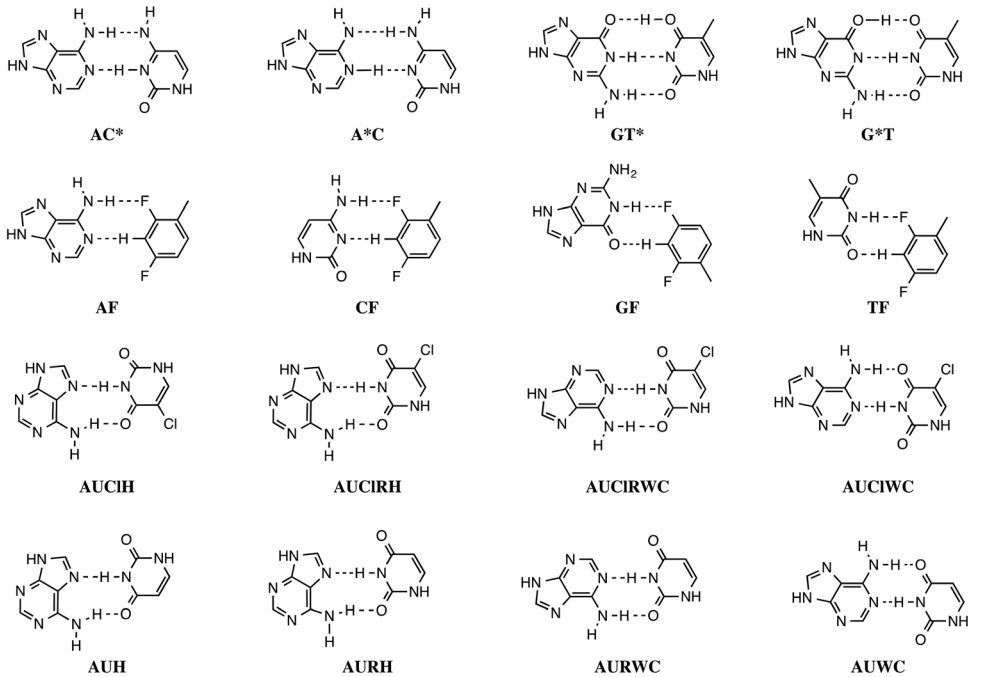

Scheme 2 Base pairs formed of DNA bases, tautomers thereof, artificial DNA bases and RNA bases.

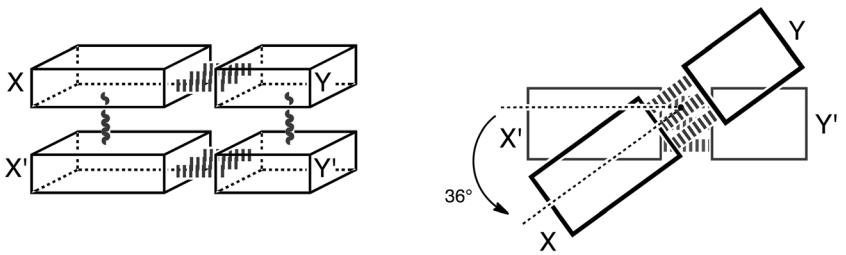

Scheme 3 Schematic presentation of the stacked base pairs XY and X′Y′ and the twist angle.

structure and bonding in the stacks of 47 base pairs, including natural, mismatched and artificial stacked base pairs. Our structural and bonding analyses are based on state-of-the-art Kohn–Sham molecular orbital theory at the BP86-D/TZ2P level. We investigate the different interactions that add to the stable structure of B-DNA: that is hydrogen-bonding, π–π stacking interactions, cross-terms (interaction between X and Y′, see Scheme 3) and the influence of these two interactions onto each other. We complement these analyses with an exploration of the role of solvation and of the twist-angle.

Computational methods

General procedure

All calculations were carried out with the ADF program[11] using dispersion-corrected density functional theory (using Grimme's DFT-D correction)[12] at the BP86-D/TZ2P level of theory.[13] Solvent effects in aqueous solution are described with the COSMO model, which takes effectively into account cavitation, internal energy and entropy effects of the solvent and yields an estimate of the Gibbs free energies.[14] The BP86-D functional was recently shown to yield hydrogen-bonding structures and energies for AT and GC Watson–Crick pairs and stacked configurations[15] that agree excellently with the best *ab initio* CCSD(T) benchmark data.[16] All systems have been optimized under C_s symmetry constraint with the aim to simulate the experimental condition B-DNA where the base pairs are nearly planar and attached to the backbone. Previously, it was shown that the difference in stability between such C_s-symmetric structures and fully optimized, non-planar geometries is very small: bond energies at the relaxed C_1 and C_s conformations differ by 0.1 kcal mol^{-1} or less (except for the GA and GG1 systems that differ 0.6 and 0.3 kcal mol^{-1}, respectively, because of the pyramidalization of the amino group).[5,17]

Bonding analyses

The bonding interactions have been further analyzed by means of the energy decomposition analysis.[18] The interaction energy ΔE_{int} corresponds to the actual energy change when the

separated bases are combined to form the base pair, and can be decomposed:

$$\Delta E_{\text{int}} = \Delta V_{\text{elstat}} + \Delta E_{\text{Pauli}} + \Delta E_{\text{oi}} + \Delta E_{\text{disp}} \quad (1)$$

Here, ΔV_{elstat} corresponds to the classical electrostatic interaction between the unperturbed charge distributions of the prepared bases and is usually attractive. The Pauli-repulsion ΔE_{Pauli} comprises the destabilizing interactions between occupied orbitals and is responsible for the steric repulsions. The orbital interaction ΔE_{oi} accounts for charge transfer (donor–acceptor interactions between occupied orbitals on one moiety with unoccupied orbitals of the other, including the HOMO–LUMO interactions) and polarization (empty/occupied orbital mixing on one fragment due to the presence of another fragment). The latter can be decomposed into the contributions from each irreducible representation of the interacting system (*i.e.* σ and π in our planar base pairs). Finally, the ΔE_{disp} term (Grimme's DFT-D correction) accounts for the dispersion interactions.[12,19]

Model systems

In this computational investigation, stacked base pairs will be considered (see Scheme 3). Equivalent base pairs (X–Y and X′–Y′) are stacked above each other with a distance of 3.4 Å between the planes of the base pairs (see Scheme 3). The calculations were done at a twist angle of 0° and 36° to understand the role of the angle in the stabilization of B-DNA. The following nomenclature is used throughout this work: a dash "–" denotes hydrogen bonding; a slash "/" denotes stacking; the prime denotes the lower base and the fragments are put between parenthesis (see Scheme 3). Thus, $\Delta E_{\pi-\pi}^{(\text{X–Y})/(\text{X′–Y′})}$ denotes the stacking interaction between two identical base pairs X–Y, and $\Delta E_{\text{HB}}^{(\text{X/X′})-(\text{Y/Y′})}$ denotes the hydrogen bonding interaction between two stacked X bases (X/X′) with two stacked Y bases (Y/Y′). The separate terms of the interactions in the stacked base pairs are represented as: $\Delta E_{\pi-\pi}^{\text{X/X′}}$ is the stacking interaction between two bases X, $\Delta E_{\text{HB}}^{\text{X–Y}}$ is the hydrogen bonding interaction between base X and base Y and $\Delta E_{\text{cross}}^{\text{X/Y′}}$ denotes the cross-term interaction between the diagonally opposite bases X and Y′ (see Scheme 3).

The cooperativity within the hydrogen bond energy of one base pair XY due to the simultaneous occurrence of the stacking can be calculated as follows (see Scheme 3):

$$\Delta\Delta E_{\text{coop}}(\text{H}) = \Delta E_{\text{HB}}^{(\text{X/X′})-(\text{Y/Y′})} - 2\Delta E_{\text{HB}}^{\text{X–Y}} - [\Delta E_{\text{cross}}^{\text{X/Y′}} + \Delta E_{\text{cross}}^{\text{X′/Y}}] \quad (2)$$

If the value of $\Delta\Delta E_{\text{coop}}(\text{H})$ is negative, the stacking reinforces the hydrogen bonding. The influence of the hydrogen bonds on the stacking interactions can be calculated as follows:

$$\Delta\Delta E_{\text{coop}}(\pi) = \Delta E_{\pi-\pi}^{(\text{X–Y})/(\text{X′–Y′})} - \Delta E_{\pi-\pi}^{\text{X/X′}} - \Delta E_{\pi-\pi}^{\text{Y/Y′}} - [\Delta E_{\text{cross}}^{\text{X/Y′}} + \Delta E_{\text{cross}}^{\text{X′/Y}}] \quad (3)$$

If the value of $\Delta\Delta E_{\text{coop}}(\pi)$ is negative the hydrogen bonds reinforce the stacking interactions. It can be easily derived (see ESI†) that for the definition of cooperativity proposed above, the following holds: $\Delta\Delta E_{\text{coop}}(\text{H}) = \Delta\Delta E_{\text{coop}}(\pi)$. Therefore we refer in the remaining text as $\Delta\Delta E_{\text{coop}}$.

Results and discussion

The series of base pairs studied comprises the natural Watson–Crick, mismatched and artificial DNA base pairs as mentioned above (see Schemes 1 and 2). To understand the stabilizing interactions in B-DNA and supramolecular systems inspired by DNA, we have analyzed a stack of two identical base pairs at a distance of 3.4 Å, X–Y/X′–Y′ (see Scheme 3). We have used for that purpose the geometries of the base pairs obtained from BP86-D/TZ2P optimizations.[5] The dimer of two base pairs is stabilized by hydrogen bonding between the bases within one layer, and stacking interactions between the bases of the different layers.

Hydrogen bonding

The hydrogen-bond interaction energies, $\Delta E_{\text{HB}}^{(\text{X/X′})-(\text{Y/Y′})}$, for all stacked systems (X–Y/X′–Y′) are calculated as the interaction between two stacked X bases and two stacked Y bases, thus X/X′ and Y/Y′ (see Tables 1 and 2). Table 1 shows the values for the series of 31 Watson–Crick and mismatched base pairs, and Table 2 encloses the values for the RNA and modified base pairs. Comparison of the calculated hydrogen bonds energies at a twist angle of 0° and 36°, reveals that they are almost equivalent with differences of less than 1.4 kcal mol^{-1}. Furthermore, we observe that the hydrogen bonds energies are almost halved when the stack is solvated by water, which is in correspondence with our previous findings for the single base pairs.[5,6,15]

To investigate if the hydrogen bond interaction energies in a stack differ from the hydrogen bond interaction energies in an isolated base pair, we compared for the gas phase situation the hydrogen bond interaction energies of the stack, $\Delta E_{\text{HB}}^{(\text{X/X′})-(\text{Y/Y′})}$, to twice the hydrogen bond interaction energies of an isolated base pair X–Y, $\Delta E_{\text{HB}}^{\text{X–Y}}$. The outcome is that the hydrogen bond interaction energies are always larger (in absolute value) in the stack (except GCRWC by 0.4 kcal mol^{-1}). For the Watson–Crick base pairs the hydrogen bonds of the stacked system amounts at a twist angle of 0° in the gas phase to −45.4 kcal mol^{-1} for ATWC and −82.0 kcal mol^{-1} for GCWC, whereas twice the hydrogen bond energy of ATWC and GCWC sums up to −41.8 kcal mol^{-1} and −73.8 kcal mol^{-1}, respectively. This can be rationalized as the values of the stack cannot be fully attributed to the hydrogen bonds alone. There are two bases per layer, so there are also interactions present between bases that are in a sense diagonally to each other, that is on opposite sides and in different layers, the so-called cross terms (see Scheme 3). These cross-terms also contribute to the "hydrogen-bond" interaction of these systems ($\Delta E_{\text{cross}}^{\text{X/Y′}}$ and $\Delta E_{\text{cross}}^{\text{X′/Y}}$). For the naturally occurring Watson–Crick base pairs these cross-terms amount to −2.6 kcal mol^{-1} and −10.0 kcal mol^{-1} for stacked ATWC and GCWC respectively at

Table 1 Stacking energy $\Delta E_{\pi-\pi}$, hydrogen bond interaction ΔE_{HB} and cross terms ΔE_{cross} (in kcal mol^{-1}) for two identical stacked bases pairs X–Y, at a twist angle of 0° and 36° [a]

	Stacking [b]					Hydrogen bonding								
	$\Delta E_{\pi-\pi}^{(X-Y)/(X'-Y')}$					$2\Delta E_{HB}^{X-Y}$	$\Delta E_{HB}^{(X/X')-(Y/Y')}$				$\Delta E_{cross}^{X/Y'} + \Delta E_{cross}^{X'/Y}$		$\Delta\Delta E_{coop}$ [c]	
	0°		36°				0°		36°					
XY	Gas	Wat	Gas	Wat	$\Delta\Delta_{gas}$	Pair Gas	Gas	Wat	Gas	Wat	0° Gas	36° Gas	0° Gas	36° Gas
Watson–Crick														
ATWC	−3.9	−5.8	−12.2	−9.8	−8.3	−41.8	−45.4	−23.8	−44.6	−23.8	−2.6	−2.0	−1.0	−0.8
GCWC	−3.0	−7.9	−9.8	−9.7	−6.8	−73.8	−82.0	−33.4	−80.8	−34.4	−10.0	−8.4	1.8	1.4
Mismatches														
AA2	−6.5	−9.7	−13.2	−10.2	−6.7	−33.8	−36.2	−19.8	−36.4	−19.8	−1.8	−2.0	−0.6	−0.6
AA3	−6.0	−9.4	−13.7	−9.7	−7.7	−28.6	−30.8	−16.2	−31.4	−16.4	−1.2	−1.6	−1.0	−1.2
AA4	−7.0	−9.5	−12.8	−10.0	−5.8	−37.0	−40.2	−21.0	−40.0	−21.2	−2.6	−2.4	−0.6	−0.6
AAx	−5.5	−8.7	−11.5	−8.3	−6.0	−18.8	−20.2	−9.2	−20.4	−9.0	−0.8	−0.8	−0.6	−0.8
AC2	−2.6	−5.8	−9.6	−8.0	−7.0	−40.6	−44.2	−17.2	−43.6	−18.2	−2.8	−2.0	−0.8	−1.0
AC4	−3.4	−6.0	−10.4	−8.1	−7.0	−43.4	−48.0	−19.0	−47.4	−19.6	−4.0	−3.4	−0.6	−0.6
ACx	−1.0	−5.5	−8.2	−7.0	−7.2	−19.8	−21.6	−7.0	−21.4	−7.8	−0.4	−0.2	−1.4	−1.4
ATH	−4.0	−6.0	−13.1	−9.5	−9.1	−40.8	−44.6	−21.6	−44.4	−21.4	−3.2	−2.8	−0.6	−0.8
ATRH	−4.0	−5.9	−12.7	−8.6	−8.7	−39.8	−43.6	−20.8	−43.2	−20.2	−3.2	−2.6	−0.6	−0.8
ATRWC	−3.8	−6.1	−11.9	−9.4	−8.1	−40.4	−44.0	−23.2	−43.2	−22.8	−2.4	−1.6	−1.2	−1.2
CC3	−1.0	−1.5	−9.3	−5.2	−8.3	−53.6	−60.8	−16.0	−60.6	−17.8	−7.8	−7.2	0.6	0.2
CCx	4.7	−3.6	−5.1	−4.8	−9.8	−22.2	−23.0	−8.6	−24.0	−8.6	−3.0	−3.4	2.2	1.6
CT5	0.9	−0.8	−7.6	−5.3	−8.6	−35.0	−38.6	−13.6	−38.2	−14.2	−2.0	−2.0	−1.6	−1.2
CT6	1.2	−1.4	−7.0	−4.6	−8.1	−32.6	−36.0	−13.8	−35.4	−13.0	−1.6	−1.2	−1.8	−1.6
GA	−6.0	−10.6	−12.8	−10.8	−6.8	−46.4	−51.8	−22.6	−51.8	−22.8	−5.6	−5.4	0.2	0.0
GA2	−3.7	−9.2	−12.4	−7.8	−8.8	−31.6	−34.4	−18.6	−34.8	−17.8	−2.0	−2.4	−0.8	−0.8
GA3	−5.1	−10.1	−12.4	−10.0	−7.3	−40.4	−44.8	−20.2	−44.8	−20.0	−3.8	−3.6	−0.6	−0.8
GC1	−0.5	−5.2	−9.6	−6.3	−9.1	−43.0	−47.6	−17.6	−47.4	−18.4	−4.6	−4.3	0.0	−0.1
GCx	−3.5	−7.6	−9.8	−8.8	−6.3	−66.0	−74.6	−26.4	−74.0	−27.2	−10.4	−9.0	1.8	1.0
GCRWC	4.4	−7.1	−2.7	−7.4	−7.1	−31.4	−31.0	−21.0	−31.8	−21.4	−2.2	−2.4	2.6	2.0
GG1	−1.5	−9.0	−10.5	−8.8	−9.1	−46.2	−50.2	−21.0	−50.8	−20.6	−6.8	−6.6	2.8	2.0
GG3	−6.8	−10.6	−14.1	−10.7	−7.3	−72.0	−82.0	−27.4	−81.6	−28.2	−12.2	−10.8	2.2	1.2
GG4	−0.9	−8.1	−10.5	−5.2	−9.6	−32.0	−35.0	−18.2	−34.8	−17.0	−1.6	−1.6	−1.4	−1.2
GGx	1.9	−9.3	−6.5	−8.1	−8.4	−31.8	−32.2	−19.0	−33.2	−18.0	−3.4	−3.8	3.0	2.4
GT2	−0.9	−6.8	−8.8	−9.0	−8.0	−43.8	−48.0	−24.2	−47.0	−23.6	−3.2	−2.2	−1.0	−1.0
GT3	−1.1	−6.2	−10.0	−9.8	−8.8	−47.2	−51.4	−23.8	−50.8	−23.8	−3.8	−3.2	−0.4	−0.4
TT3	1.2	−1.5	−9.1	−6.2	−10.2	−29.8	−32.0	−20.0	−32.4	−19.6	−1.2	−1.8	−1.0	−0.8
TT4	0.9	−1.7	−10.7	−7.4	−11.6	−33.4	−35.8	−21.4	−36.2	−20.4	−1.6	−2.2	−0.8	−0.6
TT5	1.0	−1.5	−10.0	−7.1	−11.0	−31.4	−33.8	−20.6	−34.2	−19.8	−1.4	−2.0	−1.0	−0.8

[a] Calculated at the BP86-D/TZ2P level of theory in the gas phase and in water (COSMO). [b] $\Delta\Delta_{gas}$ is the difference in stacking energy between at a twist angle of 0° and 36°. [c] See eqn (2).

a twist angle of 0° (see Tables 1 and 3). This shows the importance of the cross terms, which cannot be underestimated in such stacked systems, for which we usually only refer to the π–π stacking interactions. The cross term is always attractive in the gas-phase, and it is larger for GC-rich DNA than for AT-rich DNA. So, that adds up to an extra stabilization of the GC-rich DNA. This outcome shows that the GC rich double strands of DNA are stronger bonded not only because of their stronger hydrogen bonds, but also due to their larger cross-terms between G and C′ and between G′ and C (–5.2 and −3.2 kcal mol^{-1} respectively at a twist angle of 36°, see Table 3). Other stacked base pairs with large cross terms are GCx, GG3 and GT* (–9.0 kcal mol^{-1}, −10.8 kcal mol^{-1} and −7.6 kcal mol^{-1} at a twist angle of 36°).

After having established that the cross-terms make a large contribution to the hydrogen bonding, we want to determine if there is a cooperativity between the hydrogen bonding and the stacking interactions. Therefore, the $\Delta\Delta E_{coop}$ is calculated as the difference between the hydrogen bond energy of the stack $\Delta E_{HB}^{(X/X')-(Y/Y')}$, and the individual terms ($2\Delta E_{HB}^{X-Y} + \Delta E_{cross}^{X/Y'} + \Delta E_{cross}^{X'/Y}$). A negative value of $\Delta\Delta E_{coop}$ corresponds to cooperativity and a positive value to non-cooperative effect (see Tables 1 and 2). The largest non-cooperativity is found at a twist angle of 0° for the base pairs with a surplus of hydrogen bonds pointing in one direction. In the case of GCWC, GCRWC, GG1, GG3 and GGx the non-cooperative effect amounts to respectively 1.8, 2.6, 2.8, 2.2 and 3.0 kcal mol^{-1}. A surplus of hydrogen bonds in one direction leads to a charge accumulation on one side of the stack and a charge depletion on the other side of the stack due to the donor–acceptor interactions in the hydrogen bonds.[4] The DNA bases on top of each other will therefore repel each other slightly. This non-cooperative effect will be explained in more detail below.

The energy decomposition analysis for the hydrogen bonds between the stacked X/X′ and Y/Y′ is given in Table 4. As already observed for the base pairs alone, for the stacked

Table 2 Stacking energy $\Delta E_{\pi-\pi}$, hydrogen bond interaction ΔE_{HB} and cross terms ΔE_{cross} (in kcal mol^{-1}) for two identical stacked bases pairs X–Y, at a twist angle of 0° and 36° [a]

	Stacking[b]					Hydrogen bonding								
	$\Delta E_{\pi-\pi}^{(X-Y)/(X'-Y')}$					$2\Delta E_{HB}^{X-Y}$	$\Delta E_{HB}^{(X/X')-(Y/Y')}$				$\Delta E_{cross}^{X/Y'} + \Delta E_{cross}^{X'/Y}$		$\Delta\Delta E_{coop}$ [c]	
	0°		36°				0°		36°					
XY	Gas	Wat	Gas	Wat	$\Delta\Delta_{gas}$	Pair Gas	Gas	Wat	Gas	Wat	0° Gas	36° Gas	0° Gas	36° Gas
Lactim mismatches														
AC*	−4.3	−6.4	−10.7	−9.0	−6.5	−44.2	−47.4	−26.4	−46.8	−26.4	−2.0	−1.4	−1.2	−1.2
A*C	−3.7	−5.7	−10.3	−8.0	−6.6	−61.0	−67.2	−27.0	−66.4	−28.2	−6.8	−5.6	0.6	0.2
GT*	−3.4	−7.7	−11.5	−11.2	−8.1	−94.0	−102.2	−46.2	−100.8	−46.2	−9.4	−7.6	1.2	0.8
G*T	−2.8	−7.0	−10.9	−10.7	−8.1	−57.6	−60.4	−39.4	−59.4	−39.4	−2.6	−1.2	−0.2	−0.6
Difluorotoluene mismatches														
AF	−4.9	−6.2	−11.1	−9.7	−6.2	−11.2	−13.0	−3.6	−13.0	−4.0	−1.2	−1.2	−0.6	−0.6
CF	−0.4	−1.6	−7.3	−6.3	−6.9	−11.6	−13.6	0.8	−13.6	0.6	−1.0	−0.8	−1.0	−1.2
GF	−2.8	−6.5	−9.4	−9.4	−6.6	−16.0	−18.6	−4.4	−18.6	−4.4	−2.4	−2.2	−0.2	−0.4
TF	−0.9	−2.3	−9.5	−7.8	−8.6	−9.4	−10.8	−4.0	−11.0	−3.4	−1.0	−1.2	−0.4	−0.4
Chlorouracil and uracil mismatches														
AUClH	−4.6	−5.9	−13.2	−8.9	−8.5	−42.4	−46.6	−23.2	−46.4	−23.4	−3.6	−3.2	−0.6	−0.6
AUClRH	−4.6	−6.0	−12.5	−8.1	−7.9	−41.8	−45.8	−23.0	−45.4	−23.0	−3.4	−2.8	−1.0	−1.2
AUClRWC	−4.2	−6.6	−11.7	−8.9	−7.4	−42.6	−46.2	−25.8	−45.6	−25.6	−2.6	−1.8	−0.2	−0.4
AUClWC	−4.5	−6.1	−12.4	−9.4	−7.9	−44.0	−48.0	−25.4	−47.6	−25.8	−3.2	−2.6	−0.4	−0.4
AUH	−4.5	−6.9	−11.7	−8.8	−7.2	−41.0	−45.0	−22.6	−44.6	−22.2	−3.2	−2.6	−0.6	−0.6
AURH	−4.4	−6.6	−11.8	−8.7	−7.3	−39.8	−43.6	−21.4	−43.2	−21.4	−3.2	−2.6	−1.0	−1.2
AURWC	−4.1	−6.9	−10.8	−9.1	−6.7	−40.2	−43.6	−23.8	−42.8	−23.2	−2.2	−1.6	−0.2	−0.4
AUWC	−4.3	−6.8	−11.0	−9.2	−6.7	−42.2	−46.0	−24.6	−45.2	−24.4	−2.8	−2.0	−0.4	−0.4

[a] Calculated at the BP86-D/TZ2P level of theory in the gas phase and in water (COSMO). [b] $\Delta\Delta_{gas}$ is the difference in stacking energy between at a twist angle of 0° and 36°. [c] See eqn (2).

systems we reconfirm the importance of the covalent character of hydrogen bonds, a component (ΔE_{oi} over ΔV_{elstat} + ΔE_{oi} + ΔE_{disp}) which contributes up to 46% of all hydrogen-bonding forces in our set of model complexes.

Stacking interactions

The π–π stacking interactions present in the stacked dimers of the base pairs can be influenced by the twist angle, the solvent and hydrogen bonds. The stacking energy, $\Delta E_{\pi-\pi}^{(X-Y)/(X'-Y')}$ is calculated as the energy difference between the stacked base pairs and the individual base pairs (X–Y and X′–Y′), both in gas phase and in aqueous solution and by considering the fully parallel base pairs with a twist angle (tw) of 0°, and the natural occurring twist angle of 36° (see Tables 1 and 2). Table 1 shows the corresponding values for the series of 31 Watson–Crick and mismatched base pairs, and Table 2 encloses those for the RNA and modified base pairs.

The stacking interaction is always more attractive at a twist angle of 36° in gas phase (see Tables 1 and 2) and in water (see also Table S1 of the ESI†). *In vacuo*, the average gain in stacking energy by twisting from 0° to 36° amounts to −7.9 kcal mol^{-1}, and in water to −2.2 kcal mol^{-1} (see Tables 1 and 2). $\Delta\Delta_{gas}$ values in Tables 1 and 2 denote the energy difference between the stacking energy at a twist angle of 36° and at 0° in the gas phase. These $\Delta\Delta_{gas}$ values range from −5.8 kcal mol^{-1} to −11.6 kcal mol^{-1}.

The natural occurring DNA base pairs ATWC and GCWC will be explained in more detail, because of their biological importance. At the B-DNA twist angle and under solvated conditions, the stacking interaction is quite similar in energy for the Watson–Crick base pairs: the stacking interaction amounts to −9.8 kcal mol^{-1} for (A–T)/(A′–T′) and for (G–C)/(G′–C′) to −9.7 kcal mol^{-1}. Thus, under natural conditions (solvation and twist-angle of 36°) the stabilization to structure of B-DNA by the π–π stacking between two ATWC pairs or two GCWC pairs is equalized.

In the gas phase, the $\Delta E_{\pi-\pi}^{(X-Y)/(X'-Y')}$ amounts for AT to −12.2 kcal mol^{-1} at 36° and for GC to −9.8 kcal mol^{-1}. These values confirm our previous values obtained at the LDA/TZ2P and KT1/TZ2P levels of theory.[1d] The decomposition of this stacking interaction into the individual terms of base–base stacking interaction ($\Delta E_{\pi-\pi}^{X/X'}$) and cross terms ($\Delta E_{\pi-\pi}^{X/Y'}$) is given in Table 3. For the stacked ATWC base pair, the largest contribution to the total stacking interaction comes from the base–base stacking interaction, $\Delta E_{\pi-\pi}^{X/X'}$ (−5.4 kcal mol^{-1} for A/A′ and −3.8 kcal mol^{-1} for T/T′) and not from the cross terms (−0.9 kcal mol^{-1} and −1.1 kcal mol^{-1}). The stacking interaction for GCWC is built up in a different way. Unexpectedly, the cross terms play a much more important role than the stacking terms: $\Delta E_{\pi-\pi}^{X/X'}$ is −2.5 kcal mol^{-1} for X = G and −0.3 for X = C and the cross-terms are −5.2 kcal mol^{-1} and −3.2 kcal mol^{-1} at the natural twist angle.

The Watson–Crick base pairs improve their stacking interactions in the gas phase by −8.3 kcal mol^{-1} for ATWC and −6.8 kcal mol^{-1} for GCWC by increasing the twist angle from 0° to the natural angle of 36°. To understand how this increase

Table 3 Energy decomposition analysis of the stacking energies (in kcal mol^{-1}) of stacked Watson–Crick DNA base pairs, in the gas-phase[a]

System	Twist angle	ΔE_{Pauli}	ΔV_{elstat}	ΔE_{oi}	ΔE_{disp}	ΔE_{int}
π–π stacking between WC pairs						
(A–T)/(A′–T′)	0°	26.5	−2.5	−5.5	−22.4	−3.9
	36°	15.1	−5.2	−3.7	−18.3	−12.2
(A–T)/(A′–T′) with Me-groups optimized	0°	21.5	−1.6	−3.6	−22.1	−5.8
	36°	14.9	−5.2	−3.7	−18.3	−12.2
(G–C)/(G′–C′)	0°	20.4	1.1	−3.4	−21.2	−3.0
	36°	14.2	−2.5	−3.5	−18.0	−9.8
π–-π stacking between bases						
A/A′	0°	11.1	−0.8	−1.5	−10.8	−2.0
	36°	7.3	−2.7	−1.5	−8.5	−5.4
G/G′	0°	11.3	4.1	−2.3	−11.4	1.7
	36°	7.9	1.2	−2.2	−9.4	−2.5
T/T′	0°	15.5	0.2	−4.0	−9.9	1.8
	36°	7.5	−1.6	−2.2	−7.6	−3.8
C/C′	0°	9.4	3.6	−1.7	−7.9	3.4
	36°	5.8	1.5	−1.7	−6.0	−0.3
Cross interactions						
A/T′	0°	0.5	−0.8	−0.2	−0.9	−1.3
	36°	0.8	−0.2	−0.3	−1.2	−0.9
G/C′	0°	0.6	−3.9	−0.8	−1.0	−5.0
	36°	0.9	−4.0	−0.9	−1.2	−5.2
A′/T	0°	0.5	−0.8	−0.2	−0.9	−1.3
	36°	0.7	−0.4	−0.3	−1.1	−1.1
G′/C	0°	0.6	−3.9	−0.8	−1.0	−5.0
	36°	1.1	−2.1	−0.8	−1.4	−3.2
Sum of pairwise interactions[b]						
ATWC-0°	0°	27.6	−2.2	−5.9	−22.5	−2.8
	36°	16.3	−4.9	−4.3	−18.4	−11.2
GCWC-0°	0°	21.9	−0.1	−5.6	−21.3	−4.9
	36°	15.7	−3.4	−5.6	−18.0	−11.3

[a] Calculated at the BP86-D/TZ2P level of theory. [b] Summation of the pairwise interactions calculated for the geometries of two stacked ATWC and GCWC.

is established, we carried out an energy decomposition analysis for both ATWC and GCWC stacked systems at both twist-angles (see Table 3). The enhanced stacking interaction at the experimental twist angle is partly due to a decrease of Pauli repulsion: −11.4 kcal mol^{-1} for ATWC and −6.2 kcal mol^{-1} for GCWC (see Table 3). The electrostatic interaction and the dispersion interaction counteract each other for both systems: ΔV_{elstat} improves by twisting from 0° to 36° (–2.7 kcal mol^{-1} for ATWC and −3.6 kcal mol^{-1} for GCWC) and the dispersion interaction diminishes by 4.1 kcal mol^{-1} for ATWC and 3.2 kcal mol^{-1} for GCWC.

The stacking interaction can be divided up in the individual terms of base–base stacking (X/X′ and Y/Y′) and cross terms (X/Y′ and Y/X′), see Table 3. The energy decomposition of these individual terms reveals that the reduction of the Pauli repulsion is twice as large for the stacked T/T′ pair (−8.0 kcal mol^{-1}), than for the other three stacked systems (−3.8 kcal mol^{-1}, −3.4 kcal mol^{-1} and −3.6 kcal mol^{-1} for respectively, A/A′, G/G′ and C/C′). This larger reduction of the Pauli repulsion can be attributed to the release of the repulsive interaction between the two methyl groups of thymine bases. Relaxation of the methyl groups of thymine, while keeping the rest of the base pairs fixed, reduces the Pauli repulsion from 26.5 to 21.5 kcal mol^{-1} for a twist angle of 0° and from 15.1 to 14.9 kcal mol^{-1} for 36°. The values of the stacking interaction for AT show that it is not necessary to relax the methyl groups at a twist angle of 36° as the interaction energy and the decomposition thereof give almost the same values.

A comparison of the decomposed interaction energy at the natural twist angle for the stacked GCWC and the ATWC (with relaxed methyl groups) reveals that the larger interaction energy of the stacked ATWC pairs of −12.2 kcal mol^{-1} than of the stacked GCWC pairs (−9.8 kcal mol^{-1}) can be attributed to the more attractive electrostatic interaction of −5.2 kcal mol^{-1} for ATWC as the other terms are almost similar in size (see Table 3). This difference in electrostatic interaction can be ascribed to accumulation of electronic charge on the guanine base as it has two proton donors and one acceptor. This difference between ATWC and GCWC is only apparent in the gas phase because solvated in water these charge accumulations are stabilized leading to equal stacking interactions under natural conditions (*vide infra*).

The repulsive interactions between methyl groups at a twist angle of 0° are visible also in other stacked base pairs, particularly base pairs which contain four thymine bases such as stacked TT3, TT4 and TT5. In Table 5, the decomposition of the stacking energy for TT3 is presented (see also Table S2 of the ESI†). At the twist angle of 0°, the Pauli repulsion amounts to 30.9 kcal mol^{-1} and lowers to 12.2 kcal mol^{-1} when the base pair is twisted to 36°. Also, in this case relaxation of the methyl groups reduces the Pauli repulsion at a twist angle of 0° (21.0 kcal mol^{-1}) and results in an attractive stacking interaction at 0°. However, relaxation of the methyl groups has almost no effect at a twist angle of 36°.

The next point that we want to address is whether the π–π stacking interactions are influenced by the hydrogen bonds. At the twist angle of 0° where the influence is more pronounced, we compare the $\Delta E_{\pi-\pi}^{(X-Y)/(X'-Y')}$ with the sum of the pairwise terms. The latter does not contain the influence by hydrogen bonding (see Tables 3 and 5). For the natural occurring stacks of ATWC, the interaction energy amounts to −3.9 kcal mol^{-1} at a twist of 0° and the sum to −2.8 kcal mol^{-1}. The influence of the hydrogen bonds on the stacking interaction is thus small. Somewhat larger is the influence in the stacking interaction of the GCWC pairs. Two stacked GCWC pairs at a twist angle of 0° have an interaction energy of −3.0 kcal mol^{-1} and the individual terms sum up to −4.9 kcal mol^{-1}. The influence of the hydrogen bonds on the stacking interactions in stacked GCWC pairs is larger than in the stacked ATWC pairs. The ATWC pair has two hydrogen bonds in opposite directions, which do not lead to charge accumulations on one of the bases. The odd number of hydrogen bonds in the GCWC base pair results in an electronic charge accumulation on guanine, which disfavors the electrostatic interaction in the stacked GCWC base pairs. ΔV_{elstat} amounts to 1.1 kcal mol^{-1} for the stacked GCWC and the individual terms of the electrostatic interaction sum up to −0.1 kcal mol^{-1} (see Table 3).

Table 4 Energy decomposition analysis of the hydrogen-bond energies of stacked base pairs between X/X′ and Y/Y′, in the gas-phase and with twist angle of 0° [a]

Base pair	ΔE_{Pauli}	ΔV_{elstat}	ΔE_{oi}	ΔE_{disp}	ΔE_{bond}	Base pair	ΔE_{Pauli}	ΔV_{elstat}	ΔE_{oi}	ΔE_{disp}	ΔE_{bond}
Watson–Crick						GG4	74.4	−55.2	−42.8	−11.6	−35.0
ATWC	94.4	−73.0	−54.8	−12.0	−45.4	GGx	40.6	−39.8	−24.6	−8.2	−32.2
GCWC	117.8	−105.0	−81.0	−13.8	−82.0	GT2	82.0	−66.4	−53.2	−10.4	−48.0
Mismatches						GT3	89.4	−70.8	−58.8	−11.0	−51.4
AA2	71.0	−57.6	−39.0	−10.6	−36.2	TT3	60.4	−48.6	−35.6	−8.2	−32.0
AA3	57.0	−47.0	−30.4	−10.4	−30.8	TT4	73.0	−55.0	−44.8	−9.0	−35.8
AA4	83.2	−66.0	−46.4	−10.8	−40.2	TT5	66.8	−51.8	−40.2	−8.6	−33.8
AAx	42.4	−32.8	−21.2	−8.6	−20.2	*Lactim mismatches*					
AC2	72.6	−61.8	−43.8	−11.4	−44.2	AC*	103.4	−79.4	−58.8	−12.6	−47.4
AC4	85.4	−70.4	−51.6	−11.4	−48.0	A*C	115.4	−94.4	−75.2	−13.0	−67.2
ACx	43.6	−32.6	−23.8	−8.8	−21.6	GT*	172.0	−133.0	−127.2	−14.0	−102.2
ATH	83.4	−68.8	−48.0	−11.4	−44.6	G*T	132.6	−99.8	−78.8	−14.4	−60.4
ATRH	80.8	−67.2	−46.2	−11.2	−43.6	*Difluorotoluene mismatches*					
ATRWC	91.0	−71.0	−52.2	−12.0	−44.0	AF	22.8	−18.0	−10.4	−7.4	−13.0
CC3	89.4	−79.4	−58.8	−12.0	−60.8	CF	19.2	−14.8	−10.8	−7.2	−13.6
CCx	32.8	−29.4	−18.0	−8.4	−23.0	GF	25.6	−21.0	−14.4	−9.0	−18.6
CT5	73.2	−54.6	−46.6	−10.6	−38.6	TF	14.6	−12.4	−7.2	−5.8	−10.8
CT6	67.2	−51.0	−42.0	−10.2	−36.0	*Chlorouracil and uracil mismatches*					
GA	84.0	−68.8	−53.8	−13.4	−51.8	AUClH	86.6	−70.2	−51.4	−11.4	−46.6
GA2	68.4	−53.6	−38.0	−11.2	−34.4	AUClRH	85.4	−69.6	−50.2	−11.4	−45.8
GA3	68.2	−56.8	−43.8	−12.4	−44.8	AUClRWC	95.6	−73.2	−56.4	−12.0	−46.2
GC1	81.8	−67.6	−50.2	−11.6	−47.6	AUClWC	98.6	−75.4	−59.0	−12.2	−48.0
GCx	107.0	−96.6	−73.8	−11.2	−74.6	AUH	83.8	−69.0	−48.6	−11.2	−45.0
GCRWC	41.6	−39.0	−25.2	−8.4	−31.0	AURH	81.0	−67.0	−46.4	−11.0	−43.6
GG1	65.6	−64.0	−40.4	−11.6	−50.2	AURWC	90.8	−70.4	−52.2	−11.8	−43.6
GG3	107.0	−100.6	−75.6	−13.0	−82.0	AUWC	95.0	−73.6	−55.4	−11.8	−46.0

[a] Calculated at the BP86-D/TZ2P level of theory.

Table 5 Energy decomposition analysis of the stacking energies of stacked mismatched DNA base pairs, in the gas-phase and with twist angles of 0° and 36° [a]

XY	Twist angle	ΔE_{Pauli}	ΔV_{elstat}	ΔE_{oi}	ΔE_{disp}	ΔE_{int}
π–π stacking (X–Y)/(X′Y′)						
CCx	0°	18.6	6.4	−3.5	−16.9	4.7
	36°	12.4	0.1	−3.7	−13.9	−5.1
GCRWC	0°	20.6	8.7	−4.3	−20.6	4.4
	36°	13.0	4.6	−4.3	−15.9	−2.7
GGx	0°	22.5	8.1	−4.6	−24.2	1.9
	36°	14.4	2.2	−4.5	−18.6	−6.5
TT3	0°	30.9	−0.7	−8.1	−21.0	1.2
	36°	12.2	−2.1	−3.6	−15.6	−9.1
TT3 (Me-groups optimized)	0°	21.0	1.0	−4.2	−20.6	−2.8
	36°	12.3	−2.3	−3.6	−15.7	−9.4
Sum of pairwise interactions [b]						
CCx	0°	19.6	3.9	−3.8	−17.0	2.7
	36°	13.3	−1.8	−4.3	−13.8	−6.5
GCRWC	0°	21.6	5.6	−4.6	−20.5	1.9
	36°	13.9	2.0	−4.6	−16.0	−4.7
GGx	0°	23.4	4.7	−5.1	−24.2	−1.2
	36°	15.4	−0.7	−5.0	−18.6	−8.9
TT3	0°	31.7	−0.3	−8.2	−21.0	2.2
	36°	13.1	−1.9	−3.8	−15.6	−8.2
TT3 (Me-groups optimized)	0°	21.8	1.4	−4.4	−20.6	−1.8
	36°	13.2	−2.1	−3.8	−15.7	−8.5

[a] Calculated at the BP86-D/TZ2P level of theory. [b] Summation of the pairwise interactions calculated for the different base pairs. The pairwise interactions can be found in the ESI.

This disfavoring of the stacking interactions by the hydrogen bonds is also visible for other stacked base pairs, that is CCx, GCRWC and GGx (see Table 5, and Table S2 of the ESI†). These base pairs experience charge accumulation because they have only one hydrogen bond (CCx) or two hydrogen bonds in the same direction (GCRWC and GGx) between the bases. The numbers for the stacked GGx are the most illustrative. The stacking interaction energy is repulsive for the stacked GGx at a twist angle of 0° by 1.9 kcal mol^{-1}, whereas the sum of the individual terms is attractive by 1.2 kcal mol^{-1}: a difference of 3.1 kcal mol^{-1}. Also in this case, solvation in water will stabilize the charge accumulations.

Conclusions

The cohesion between B-DNA's single strands is not only determined by Watson–Crick hydrogen bonding but also by the diagonal interactions (cross terms) between a base in one base pair and the opposite base in the next base pair in the stack. These cross terms are particularly stabilizing between stacks of GC pairs which further reinforces the stability of GC-rich sequences which already benefit from stronger Watson–Crick hydrogen bonding (*cf.* Barone *et al.*[20]). This follows from our quantum chemical analyses of a series of 47 stacked dimers of Watson–Crick, mismatched and modified DNA base pairs, based on using dispersion-corrected density functional theory (DFT-D).

Furthermore, solvation not only weakens but also equalizes both Watson–Crick hydrogen bonding in AT and GC base pairs as well as the π–π stacking interaction between two AT pairs and that between two GC pairs. In the gas phase, stacked GC pairs are involved in a significantly stronger stacking interaction than stacked AT pairs. In the condensed-phase, solvation stabilizes individual GC pairs more strongly than AT pairs because Watson–Crick pairing leads to a net charge separation in the former that benefits more from interaction with the solvent medium.

Interestingly, the experimental twist angle of 36° is crucial for the stability of B-DNA: it leads to a stabilization of around 8 kcal mol^{-1} compared to a twist angle of 0°. The increase in stabilization is mainly attributed to a reduction of Pauli repulsion between the π electrons of the aromatic bases and, in the case of thymine, the C–H bonds of the methyl substituents. Note that these Pauli repulsion effects derive from the existence of a non-negligible π–π overlap. This is exactly the overlap that is also behind DNA's capability to conduct holes after ionization.[21]

Acknowledgements

We thank the following organizations for financial support: the HPC-Europa2 Transnational Access program of the European Union, the Netherlands Organization for Scientific Research (NWO), the Ministerio de Ciencia e Innovación (MICINN, project number CTQ2011-25086), the DIUE of the Generalitat de Catalunya (project number 2009SGR528), the Netherlands National Research School Combination – Catalysis (NRSC-C), and the European Fund for Regional Development (FEDER, grant UNGI08-4E-003). Excellent service by the Amsterdam (SURFsara) and Barcelona (BSC-CNS) supercomputing centers is gratefully acknowledged.

References

1 (*a*) J. Cerny, M. Kabelac and P. Hobza, *J. Am. Chem. Soc.*, 2008, **130**, 16055–16059; (*b*) C. D. M. Churchill, L. Navarro-Whyte, L. R. Rutledge and S. D. Wetmore, *Phys. Chem. Chem. Phys.*, 2009, **11**, 10657–10670; (*c*) C. D. Sherrill, *Acc. Chem. Res.*, 2013, **46**, 1020–1028; (*d*) M. Swart, T. van der Wijst, C. Fonseca Guerra and F. M. Bickelhaupt, *J. Mol. Model*, 2007, **13**, 1245–1257.

2 J. Poater, M. Swart, C. Fonseca Guerra and F. M. Bickelhaupt, *Chem. Commun.*, 2011, **47**, 7326–7328.

3 J. D. Watson and F. H. C. Crick, *Nature*, 1953, **171**, 737–738.

4 (*a*) C. Fonseca Guerra, T. van der Wijst and F. M. Bickelhaupt, *Chem. – Eur. J.*, 2006, **12**, 3032–3042; (*b*) C. Fonseca Guerra, F. M. Bickelhaupt and E. J. Baerends, *Cryst. Growth Des.*, 2002, **2**, 239–245; (*c*) C. Fonseca Guerra, T. van der Wijst and F. M. Bickelhaupt, *Struct. Chem.*, 2005, **16**, 211–221; (*d*) C. Greve, N. K. Preketes, H. Fidder, R. Costard, B. Koeppe, I. A. Heisler, S. Mukamel, F. Temps, E. T. J. Nibbering and T. Elsaesser, *J. Phys. Chem. A*, 2013, **117**, 594–606; (*e*) B. Koeppe, E. T. J. Nibbering and P. M. Tolstoy, *Z. Phys. Chem.*, 2013, **227**, 723–749; (*f*) H. Fidder, M. Yang, E. T. J. Nibbering, T. Elsaesser, K. Röttger and F. Temps, *J. Phys. Chem. A*, 2013, **117**, 845–854.

5 J. Poater, M. Swart, C. Fonseca Guerra and F. M. Bickelhaupt, *Comput. Theor. Chem.*, 2012, **998**, 57–63.

6 C. Fonseca Guerra, H. Zijlstra, G. Paragi and F. M. Bickelhaupt, *Chem. – Eur. J.*, 2011, **17**, 12612–12622.

7 V. I. Danilov, V. M. Anisimov, N. Kurita and D. Hovorun, *Chem. Phys. Lett.*, 2005, **412**, 285–293.

8 (*a*) K. M. Guckian, T. R. Krugh and E. T. Kool, *J. Am. Chem. Soc.*, 2000, **122**, 6841–6847; (*b*) E. T. Kool, J. C. Morales and K. M. Guckian, *Angew. Chem., Int. Ed.*, 2000, **39**, 990–1009; (*c*) J. C. Morales and E. T. Kool, *J. Am. Chem. Soc.*, 2000, **122**, 1001–1007.

9 (*a*) C. Fonseca Guerra and F. M. Bickelhaupt, *Angew. Chem., Int. Ed.*, 2002, **41**, 2092–2095; (*b*) C. Fonseca Guerra, F. M. Bickelhaupt and E. J. Baerends, *ChemPhysChem*, 2004, **5**, 481–487.

10 (*a*) P. Marlière, J. Patrouix, V. Döring, P. Herdewijn, S. Tricot, S. Cruveiller, M. Bouzon and R. Mutzel, *Angew. Chem., Int. Ed.*, 2011, **50**, 7109–7114; (*b*) C. G. Acevedo Rocha and N. Budisa, *Angew. Chem., Int. Ed.*, 2011, **50**, 6960–6962.

11 (*a*) G. te Velde, F. M. Bickelhaupt, E. J. Baerends, C. Fonseca Guerra, S. J. A. van Gisbergen, J. G. Snijders and T. Ziegler, *J. Comput. Chem.*, 2001, **22**, 931–967; (*b*) C. Fonseca Guerra, J. G. Snijders, G. te Velde and E. J. Baerends, *Theor. Chem. Acc.*, 1998, **99**, 391–403.

12 S. Grimme, *J. Comput. Chem.*, 2006, **27**, 1787–1799.

13 (*a*) A. D. Becke, *J. Chem. Phys.*, 1986, **84**, 4524–4529; (*b*) A. D. Becke, *Phys. Rev. A*, 1988, **38**, 3098–3100; (*c*) J. P. Perdew, *Phys. Rev. B: Condens. Matter*, 1986, **33**, 8822–8824; (*d*) S. H. Vosko, L. Wilk and M. Nusair, *Can. J. Phys.*, 1980, **58**, 1200–1211.

14 (*a*) A. Klamt and G. Schüürmann, *J. Chem. Soc., Perkin Trans. 2*, 1993, 799–805; (*b*) C. C. Pye and T. Ziegler, *Theor. Chem. Acc.*, 1999, **101**, 396–408; (*c*) M. Swart, E. Rösler and F. M. Bickelhaupt, *Eur. J. Inorg. Chem.*, 2007, 3646–3654.

15 (*a*) C. Fonseca Guerra, T. van der Wijst, J. Poater, M. Swart and F. M. Bickelhaupt, *Theor. Chem. Acc.*, 2010, **125**, 245–252; (*b*) T. van der Wijst, C. Fonseca Guerra, M. Swart, F. M. Bickelhaupt and B. Lippert, *Angew. Chem., Int. Ed.*, 2009, **48**, 3285–3287.

16 J. Sponer, P. Jurecka and P. Hobza, *J. Am. Chem. Soc.*, 2004, **126**, 10142–10151.

17 (*a*) J. Sponer, J. Leszczynski and P. Hobza, *J. Phys. Chem.*, 1996, **100**, 1965–1974; (*b*) C. Fonseca Guerra, F. M. Bickelhaupt, J. G. Snijders and E. J. Baerends, *J. Am. Chem. Soc.*, 2000, **122**, 4117–4128.

18 (*a*) F. M. Bickelhaupt and E. J. Baerends, ed. K. B. Lipkowitz and D. B. Boyd, Wiley-VCH, New York,

2000, vol. 15, pp. 1–86; (*b*) K. Kitaura and K. Morokuma, *Int. J. Quantum Chem.*, 1976, **10**, 325–340; (*c*) K. Morokuma, *J. Chem. Phys.*, 1971, **55**, 1236–1244; (*d*) J. Poater, M. Solà and F. M. Bickelhaupt, *Chem. – Eur. J.*, 2006, **12**, 2889–2895; (*e*) T. Ziegler and A. Rauk, *Theor. Chim. Acta*, 1977, **46**, 1–10; (*f*) T. Ziegler and A. Rauk, *Inorg. Chem.*, 1979, **18**, 1558–1565.

19 S. Grimme, *J. Comput. Chem.*, 2004, **25**, 1463–1473.

20 G. Barone, C. Fonseca Guerra and F. M. Bickelhaupt, *ChemistryOpen*, 2013, **2**, 186–193.

21 K. Senthilkumar, F. C. Grozema, C. Fonseca Guerra, F. M. Bickelhaupt, F. D. Lewis, Y. A. Berlin, M. A. Ratner and L. D. A. Siebbeles, *J. Am. Chem. Soc.*, 2005, **127**, 14894–14903.